Status of next-generation $\Lambda_b \to p, \Lambda, \Lambda_c$ form-factor calculations

Stefan Meinel

Processes of interest

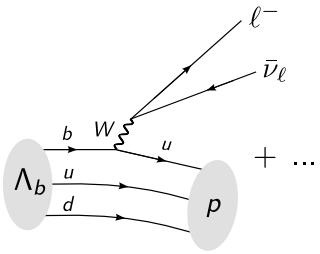

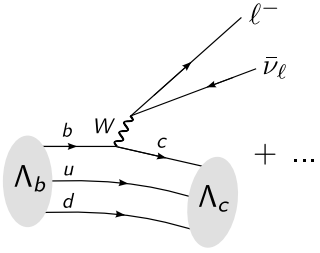

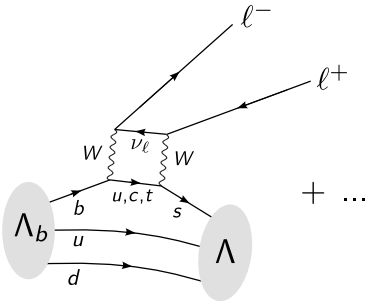

Form factor definitions

Current	Form factors
Vector	f_0, f_+, $f_\perp$
Axial vector	g_0, g_+, $g_\perp$
Tensor	h_+, $h_\perp$, $\widetilde{h}_+$, $\widetilde{h}_\perp$

Example:

$$\begin{aligned}\langle \Lambda_c(p',s')|\bar{c}\gamma^\mu\gamma_5 b|\Lambda_b(p,s)\rangle \;=\; & -\bar{u}_{\Lambda_c}(p',s')\,\gamma_5\Bigg[(m_{\Lambda_b}+m_{\Lambda_c})\frac{q^\mu}{q^2}\,g_0^{\Lambda_b\to\Lambda_c}(q^2) \\ & + \frac{m_{\Lambda_b}-m_{\Lambda_c}}{s_-}\left(p^\mu+p'^\mu-(m^2_{\Lambda_b}-m^2_{\Lambda_c})\frac{q^\mu}{q^2}\right)g_+^{\Lambda_b\to\Lambda_c}(q^2) \\ & + \left(\gamma^\mu+\frac{2m_{\Lambda_c}}{s_-}p^\mu-\frac{2m_{\Lambda_b}}{s_-}p'^\mu\right)g_\perp^{\Lambda_b\to\Lambda_c}(q^2)\Bigg]u_{\Lambda_b}(p,s)\end{aligned}$$

where $q = p - p'$ and $s_\pm = (m_{\Lambda_b} \pm m_{\Lambda_c})^2 - q^2$ [T. Feldmann, M. W. Y. Yip, 1111.1844/PRD 2012]

2015 lattice-QCD results for the $\Lambda_b \to p$ form factors

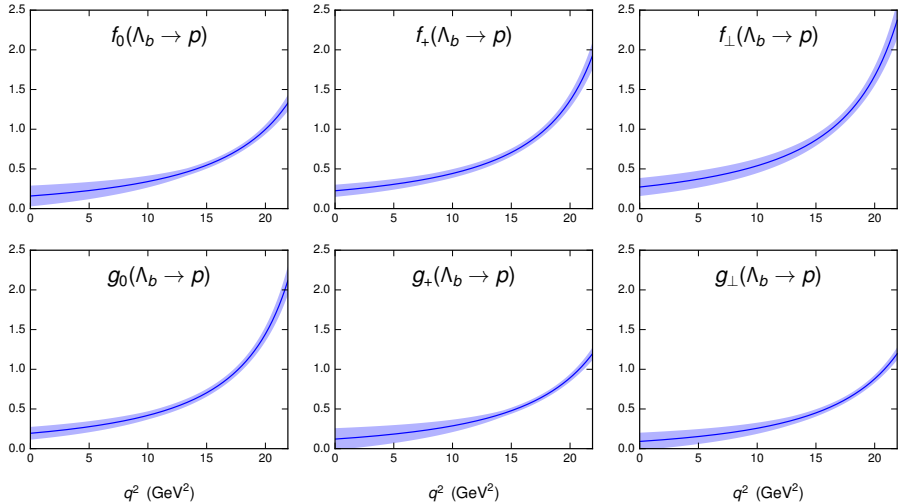

[W. Detmold, C. Lehner, S. Meinel, 1503.01421/ PRD 2015]

2015 lattice-QCD results for the $\Lambda_b \to \Lambda_c$ form factors

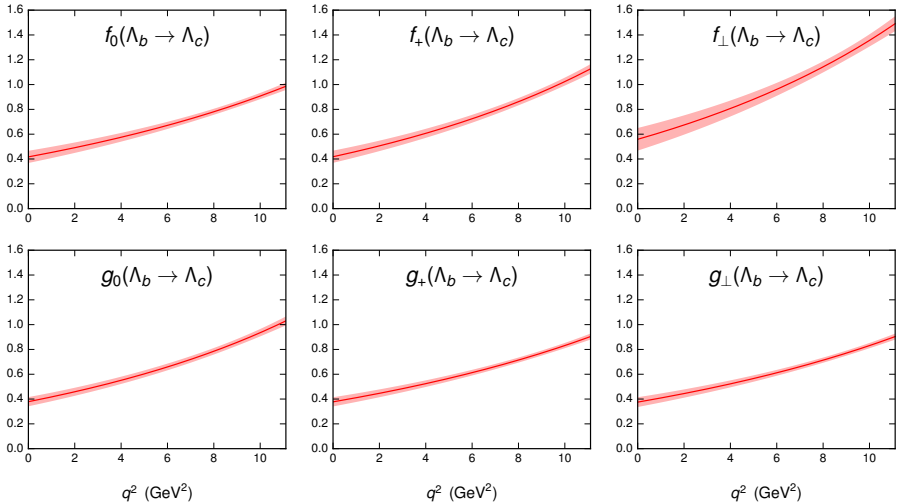

[W. Detmold, C. Lehner, S. Meinel, 1503.01421/ PRD 2015]

2016 lattice-QCD results for the $\Lambda_b \to \Lambda$ form factors

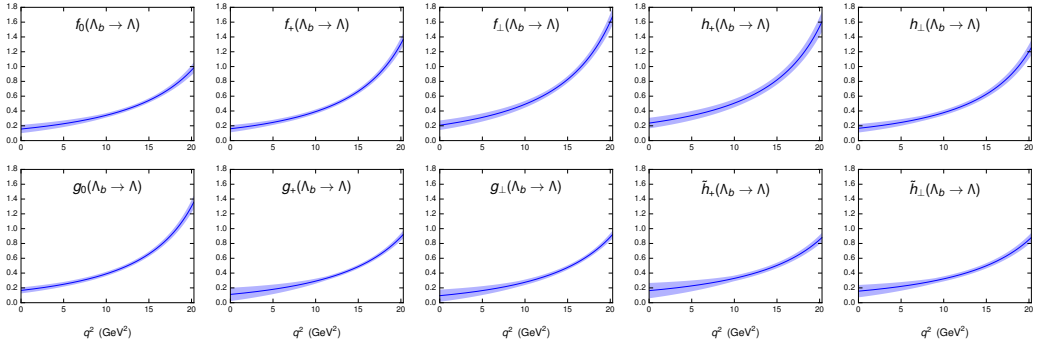

[W. Detmold, S. Meinel, 1602.01399/PRD 2016]

Applications of the $\Lambda_b \to p$ and $\Lambda_b \to \Lambda_c$ form factors

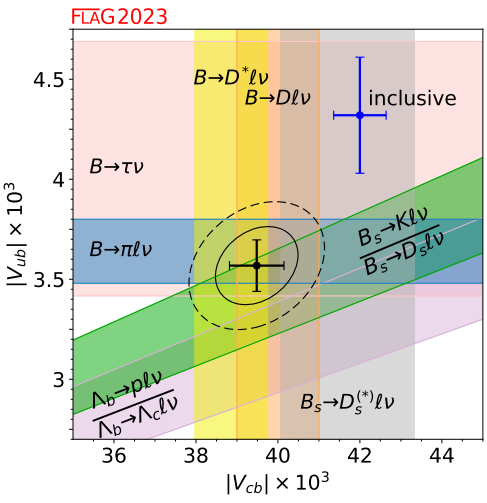

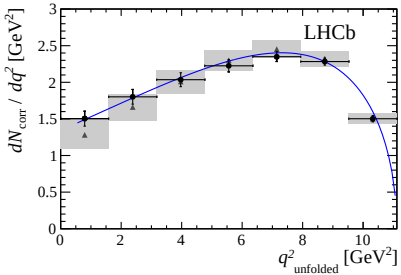

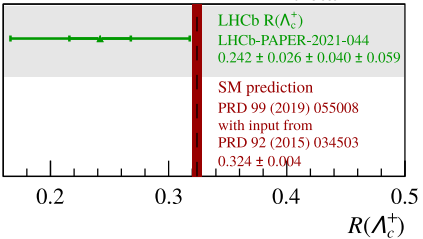

LHCb results: 1504.01568/Nature Phys. 2015; 1709.01920/PRD 2017; 2201.03497/PRL 2022

Applications of the $\Lambda_b \to \Lambda$ form factors

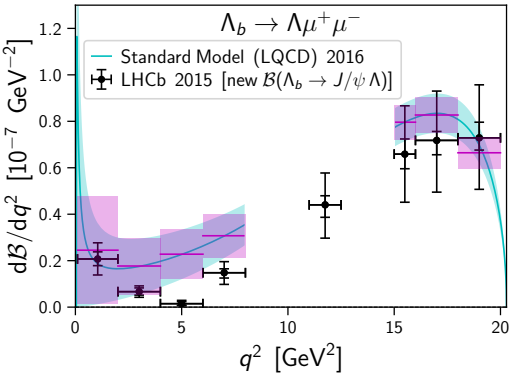

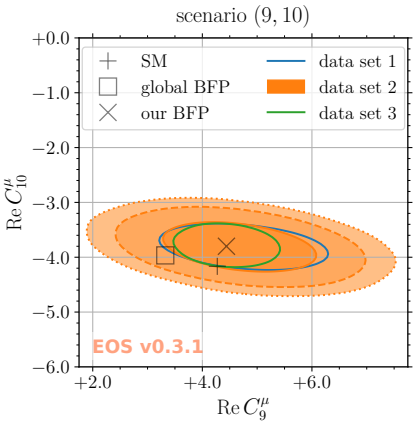

[T. Blake, S. Meinel, D. van Dyk, 1912.05811/PRD 2020]

LHCb results: 1503.07138/JHEP 2015; 1808.00264/JHEP 2018

The need for higher precision form factors

- For some quantities, e.g. $\frac{\mathrm{d}\mathcal{B}}{\mathrm{d}q^2}(\Lambda_b \to \Lambda\mu^+\mu^-)$ at low q^2, the experimental uncertainties are already smaller than the theory uncertainties.

- Substantial reductions in experimental uncertainties for all processes are expected through the continued operation of the LHC:

[Figure from 2208.05403]

For example, for $|V_{ub}/V_{cb}|$ from Λ_b decays, LHCb expects to reach 2% precision with 50 fb^{-1} [J. Albrecht *et al.*, 1709.10308], but the 2015 lattice uncertainty is 5%.

Lattice actions and ensembles

- Gluons: Iwasaki action
- u, d, s quarks: domain-wall action
- Gauge-field ensembles generated by RBC/UKQCD
- b and c quarks: anisotropic clover actions

Parameters of the 2015/2016 calculations

Label	$N_s^3 \times N_t$	β	$am_{u,d}^{(\mathrm{sea})}$	$am_{u,d}^{(\mathrm{val})}$	$am_s^{(\mathrm{sea})}$	$am_s^{(\mathrm{val})}$	a [fm]	$m_\pi^{(\mathrm{sea})}$ [MeV]	$m_\pi^{(\mathrm{val})}$ [MeV]	Samples
C14	$24^3 \times 64$	2.13	0.005	0.001	0.04	0.04	≈ 0.111	≈ 340	≈ 250	2672
C24	$24^3 \times 64$	2.13	0.005	0.002	0.04	0.04	≈ 0.111	≈ 340	≈ 270	2676
C54	$24^3 \times 64$	2.13	0.005	0.005	0.04	0.04	≈ 0.111	≈ 340	≈ 340	2782
C53	$24^3 \times 64$	2.13	0.005	0.005	0.04	0.03	≈ 0.111	≈ 340	≈ 340	1205
F23	$32^3 \times 64$	2.25	0.004	0.002	0.03	0.03	≈ 0.083	≈ 304	≈ 230	1907
F43	$32^3 \times 64$	2.25	0.004	0.004	0.03	0.03	≈ 0.083	≈ 304	≈ 304	1917
F63	$32^3 \times 64$	2.25	0.006	0.006	0.03	0.03	≈ 0.083	≈ 361	≈ 361	2782

These data sets come from three ensembles only. The red color indicates $m_{u,d}^{(\mathrm{val})} < m_{u,d}^{(\mathrm{sea})}$, leading to small $m_\pi^{(\mathrm{val})} L$ and making finite-volume errors the dominant systematic uncertainty.

Parameters of the next-generation calculations

Label	$N_s^3 \times N_t$	β	$am_{u,d}^{(\mathrm{sea,val})}$	$am_s^{(\mathrm{sea})}$	$am_s^{(\mathrm{val})}$	a [fm]	$m_\pi^{(\mathrm{sea,val})}$ [MeV]	Samples
CP	$48^3 \times 96$	2.13	0.00078	0.0362	0.0362	≈ 0.114	≈ 139	80 ex, 2560 sl
C005LV	$32^3 \times 64$	2.13	0.005	0.04	0.0323	≈ 0.111	≈ 340	186 ex, 5022 sl
C005	$24^3 \times 64$	2.13	0.005	0.04	0.0323	≈ 0.111	≈ 340	311 ex, 4976 sl
F004	$32^3 \times 64$	2.25	0.004	0.03	0.0248	≈ 0.083	≈ 304	251 ex, 4016 sl
F006	$32^3 \times 64$	2.25	0.006	0.03	0.0248	≈ 0.083	≈ 361	223 ex, 3568 sl
F1M	$48^3 \times 96$	2.31	0.002144	0.02144	0.02217	≈ 0.073	≈ 232	113 ex, 3616 sl

Six different ensembles, all data sets use $m_{u,d}^{(\mathrm{val})} = m_{u,d}^{(\mathrm{sea})}$. Now using physical $am_s^{(\mathrm{val})}$.

All propagators have been newly computed with improved source smearing, and using all-mode averaging [E. Shintani *et al.*, 1402.0244/PRD 2015].

Heavy-quark action parameters

$$S_Q = a^4 \sum_x \bar{Q} \left[m_Q + \gamma_0 \nabla_0 - \frac{a}{2} \nabla_0^{(2)} + \nu \sum_{i=1}^{3} \left(\gamma_i \nabla_i - \frac{a}{2} \nabla_i^{(2)} \right) - c_E \frac{a}{2} \sum_{i=1}^{3} \sigma_{0i} F_{0i} - c_B \frac{a}{4} \sum_{i,j=1}^{3} \sigma_{ij} F_{ij} \right] Q$$

- In the 2015/2016 Λ_b calculations, I used bottom parameters from RBC/UKQCD [1206.2554/PRD 2012], tuned using the $B_s^{(*)}$ dispersion relation and hyperfine splitting, and charm parameters from Z. Brown *et al.* [1409.0497/PRD 2014], tuned using the charmonium dispersion relation (and PT for c_E, c_B)

Parameter	C005/C01	F004/F006/F008
$am_Q^{(b)}$	8.45	3.99
$\nu^{(b)}$	3.1	1.93
$c_{E,B}^{(b)}$	5.8	3.57
$am_Q^{(c)}$	0.1214	−0.0045
$\nu^{(c)}$	1.2362	1.1281
$c_E^{(c)}$	1.6650	1.5311
$c_B^{(c)}$	1.8409	1.6232

*RBC/UKQCD use the notation $m_0 = m_Q$, $\zeta = \nu$, $c_P = c_{E,B}$

Heavy-quark action parameters

$$S_Q = a^4 \sum_x \bar{Q} \left[m_Q + \gamma_0 \nabla_0 - \frac{a}{2} \nabla_0^{(2)} + \nu \sum_{i=1}^{3} \left(\gamma_i \nabla_i - \frac{a}{2} \nabla_i^{(2)} \right) - c_E \frac{a}{2} \sum_{i=1}^{3} \sigma_{0i} F_{0i} - c_B \frac{a}{4} \sum_{i,j=1}^{3} \sigma_{ij} F_{ij} \right] Q$$

- Following improved determinations of the lattice spacings [T. Blum *et al.*, 1411.7017/PRD 2016], RBC/UKQCD re-tuned the bottom parameters in 2017, finding
  [O. Witzel, private communication 2017, and J. Flynn *et al.*, 2303.11280/PRD 2023]

Parameter	C005/C01	F004/F006/F008
$am_Q^{(b)}$	7.471(51)(75)(82)(45)	3.485(25)(38)(45)(31)
$\nu^{(b)}$	2.929(63)(100)(15)(03)	1.760(30)(58)(07)(02)
$c_{E,B}^{(b)}$	4.92(13)(28)(07)(24)	3.06(07)(18)(05)(15)

Heavy-quark action parameters

- I computed and analyzed my own $B_s^{(*)}$ two-point functions for several choices of bottom action parameters, giving the following results ($E_{B_s^{(*)}}$ values listed here are at $\mathbf{p} = 0$, i.e., = rest masses):

Ensemble	am_Q	ν	$c_{E,B}$	aE_{B_s}	E_{B_s} [GeV]	$c^2_{B_s}$	$aE_{B_s^*} - aE_{B_s}$	$E_{B_s^*} - E_{B_s}$ [MeV]
CP	8.45	3.1	5.8	3.1084(13)	5.376(12)	0.914(13)	0.0288(13)	49.8(2.3)
CP	8.1476	3.3743	5.3944	3.1025(12)	5.366(12)	1.001(14)	0.0282(13)	48.8(2.3)
C005	7.42	2.92	4.86	3.00324(81)	5.360(15)	0.9184(89)	0.02602(52)	46.44(94)
C005	7.471	2.929	4.92	3.00801(81)	5.369(15)	0.9184(89)	0.02616(53)	46.69(95)
C005	7.9	2.929	4.92	3.05463(85)	5.452(15)	0.8895(91)	0.02482(53)	44.29(96)
C005	7.471	2.929	6	2.97872(77)	5.316(15)	0.9399(85)	0.03165(58)	56.5(1.1)
C005	7.471	3.3	4.92	3.03049(75)	5.409(15)	1.0186(89)	0.02665(48)	47.56(86)
C005	7.3258	3.1918	4.9625	3.00695(75)	5.367(15)	1.0013(88)	0.02719(49)	48.52(88)
F004	3.485	1.76	3.06	2.25010(82)	5.363(19)	0.855(12)	0.02053(62)	48.9(1.5)
F004	3.3	1.76	3.06	2.20958(79)	5.266(19)	0.877(12)	0.02148(61)	51.2(1.5)
F004	3.485	1.76	3.7	2.21551(78)	5.280(19)	0.877(12)	0.02468(68)	58.8(1.6)
F004	3.485	2.2	3.06	2.29690(70)	5.474(20)	1.047(12)	0.02126(51)	50.7(1.2)
F004	3.2823	2.0600	2.7960	2.25175(71)	5.366(19)	1.004(12)	0.02046(51)	48.8(1.2)
F1M	2.4538	1.7563	2.6522	1.97455(85)	5.347(20)	0.960(16)	0.01876(79)	50.8(2.2)
F1M	2.55	1.7563	2.6522	2.00012(88)	5.416(20)	0.943(17)	0.01821(81)	49.3(2.2)
F1M	2.4538	2	2.6522	2.00698(75)	5.435(20)	1.089(16)	0.01926(70)	52.2(1.9)
F1M	2.4538	1.7563	3.1	1.94472(81)	5.266(20)	0.983(16)	0.02151(83)	58.3(2.3)
F1M	2.3867	1.8323	2.4262	1.98009(81)	5.362(20)	1.003(16)	0.01799(73)	48.7(2.0)

The central values of the new RBC/UKQCD parameters (red) yield $c^2 = M_{\text{rest}}/M_{\text{kin}}$ values about 10-15 percent below 1. See the extra slides for my proposed explanation.

I used the values in green for the next-generation computations of Λ_b decay form factors.

Heavy-quark action parameters

- Similarly, I performed a new tuning of the charm parameters, now using $D_s^{(*)}$ two-point functions (same method as for bottom), and used the values shown in green.

Ensemble	am_Q	ν	$c_{E,B}$	aE_{D_s}	E_{D_s} [GeV]	$c^2_{D_s}$	$aE_{D_s^*} - aE_{D_s}$	$E_{D_s^*} - E_{D_s}$ [MeV]
CP	0.14752	1.1928	1.7784	1.12144(43)	1.9395(43)	1.0075(52)	0.07903(59)	136.7(1.1)
CP	0.27077	1.1879	2.0714	1.13419(43)	1.9616(44)	1.0008(51)	0.08353(63)	144.5(1.1)
CP	0.27514	1.1883	2.0712	1.13804(43)	1.9682(44)	1.0000(51)	0.08317(63)	143.8(1.1)
C005	0.11360	1.2045	1.7936	1.08504(53)	1.9366(55)	1.0078(95)	0.08152(80)	145.5(1.5)
C005	0.11360	1.2045	1.72	1.10561(55)	1.9733(56)	1.0019(97)	0.07796(79)	139.1(1.5)
C005	0.11360	1.13	1.7936	1.04096(53)	1.8579(53)	0.9646(89)	0.08375(82)	149.5(1.5)
C005	0.14	1.2045	1.7936	1.10676(55)	1.9753(56)	1.0018(96)	0.07934(80)	141.6(1.5)
C005	0.15410	1.2004	1.8407	1.10274(54)	1.9682(56)	1.0001(95)	0.08057(81)	143.8(1.5)
F004	−0.01750	1.1039	1.5884	0.81570(39)	1.9441(71)	1.003(10)	0.06339(84)	151.1(2.1)
F004	−0.01750	1.1039	1.51	0.84109(41)	2.0046(73)	0.999(11)	0.05992(83)	142.8(2.0)
F004	−0.01750	1.05	1.5884	0.78075(39)	1.8608(68)	0.9674(99)	0.06513(85)	155.2(2.1)
F004	0.01	1.1039	1.5884	0.84309(40)	2.0093(73)	0.998(11)	0.06090(84)	145.1(2.1)
F004	−0.05167	1.1021	1.4483	0.82583(40)	1.9682(72)	1.000(11)	0.06032(82)	143.8(2.0)
F1M	−0.01508	1.0635	1.6094	0.72535(35)	1.9643(73)	0.9766(91)	0.05356(84)	145.0(2.3)
F1M	0.005	1.0635	1.6094	0.74696(38)	2.0228(75)	0.972(10)	0.05181(86)	140.3(2.4)
F1M	−0.01508	1.09	1.6094	0.74250(37)	2.0107(75)	0.994(10)	0.05274(84)	142.8(2.3)
F1M	−0.01508	1.0635	1.7	0.69066(29)	1.8703(69)	0.9844(80)	0.05757(82)	155.9(2.3)
F1M	−0.05874	1.0941	1.5345	0.72459(34)	1.9622(73)	1.0007(93)	0.05339(81)	144.6(2.3)

Renormalization and improvement of weak currents

In the preliminary analysis shown in the following, I used the "mostly nonperturbative method" to renormalize the currents (same method as used 2015/2016):

$$J_\Gamma = \sqrt{Z_V^{qq}\, Z_V^{QQ}}\ \rho_\Gamma \left[\bar{q}\,\Gamma\, Q + \mathcal{O}(a)\right],$$

where

- ■ = nonperturbative renormalization factors of $\bar{q}\gamma^0 q$ and $\bar{Q}\gamma^0 Q$,
- ■ = one-loop residual-matching and $O(a)$-improvement coefficients.

[S. Hashimoto *et al.*, hep-ph/9906376/PRD 1999; A. El-Khadra *et al.*, hep-ph/0101023/PRD 2001]

Renormalization and improvement of weak currents

I newly determined Z_V^{cc}, Z_V^{bb} for my choice of heavy-quark parameters using ratios of zero-momentum D_s, B_s two-point and three-point functions. This is illustrated for the F004 ensemble here.

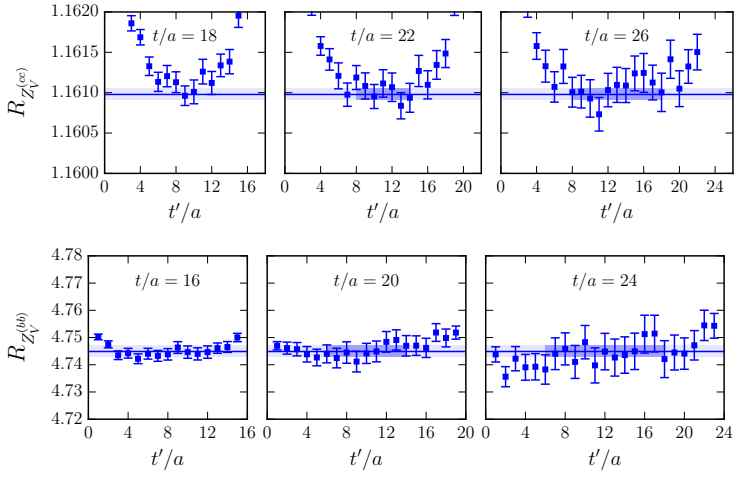

Renormalization and improvement of weak currents

Shown here are my results for Z_V^{cc} and Z_V^{bb}, along with the values I currently use for Z_V^{ll}.

Ensemble	Z_V^{ll}	Z_V^{cc}	Z_V^{bb}
CP	0.71076(25) [1]	1.40756(17)	9.9128(81)
C005, C005LV	0.71273(26) [1]	1.35761(16)	9.0631(84)
F004, F006	0.7440(18) [1]	1.160978(74)	4.7449(21)
F1M	0.761125(19) (Z_A, F1S) [2]	1.112316(61)	3.7777(23)

[1] RBC/UKQCD, 1411.7017/PRD 2016
[2] RBC/UKQCD, 1701.02644/JHEP 2017

For the residual-matching and $O(a)$-improvement coefficients in the preliminary analysis, I still use Christoph Lehner's 2012-2015 results, which were computed for the old heavy-quark-action parameters. For the CP ensemble, I currently use the same values as for C005. For F1M, I extrapolated Christoph's results linearly in the lattice spacing.

Extraction of the form factors from correlation functions

Each form factor f is obtained from the large-t limit (t = source-sink separation) of

$$R_f = \sqrt{(\text{kinematic factors}) \times \frac{\langle u\,d\,q \rangle_{t'} \times \langle u\,d\,b \rangle_{t-t'}}{\langle u\,d\,b \rangle_{t'} \times \langle u\,d\,q \rangle_{t-t'}}}$$

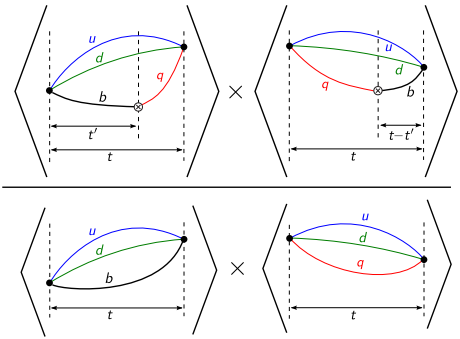

where I am setting $t' = t/2$.

Extraction of the form factors from correlation functions

Shown here are examples of preliminary fits of $R_{g_0}(t)$ used to extract g_0:

$g_0(\Lambda_b \to \Lambda)$, $|\mathbf{p}'|^2 = 4\,(2\pi/L)^2$, CP ensemble

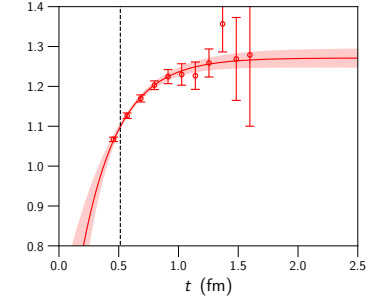

$g_0(\Lambda_b \to \Lambda)$, $|\mathbf{p}'|^2 = 2\,(2\pi/L)^2$, F1M ensemble

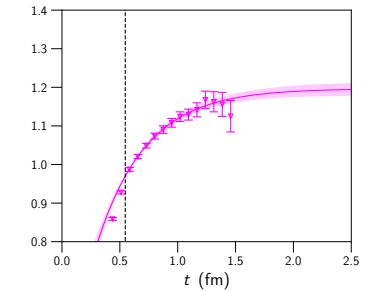

I am still working on the fits, so I will just compare the data points for $R_f(t)$ to the 2015/2016 results in the following. To keep it brief, I'll only show one kinematic point.

Recall that the interpolating-field smearing parameters are also different compared to 2015/2016.

Preliminary results: $\Lambda_b \to \Lambda_c$

$$|\mathbf{p}'|^2 = \left\{ \begin{array}{ll} 3 \cdot (2\pi/L)^2 & \text{for C005, F004, F006,} \\ 12 \cdot (2\pi/L)^2 & \text{for CP,} \\ 5 \cdot (2\pi/L)^2 & \text{for C005LV, F1M} \end{array} \right\} \approx (0.8\ \text{GeV})^2$$

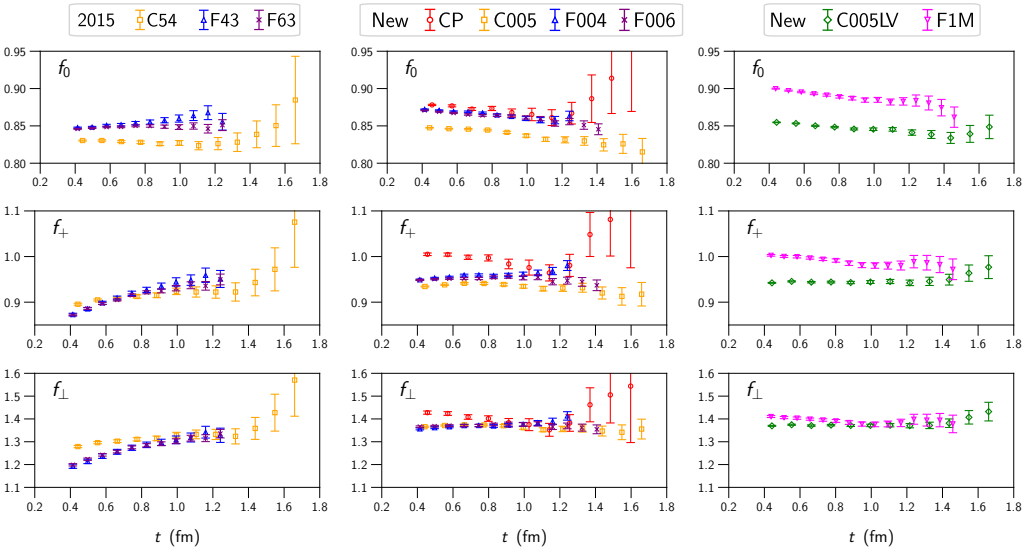

Preliminary results: $\Lambda_b \to \Lambda_c$

$$|\mathbf{p}'|^2 = \left\{ \begin{array}{ll} 3 \cdot (2\pi/L)^2 & \text{for C005, F004, F006,} \\ 12 \cdot (2\pi/L)^2 & \text{for CP,} \\ 5 \cdot (2\pi/L)^2 & \text{for C005LV, F1M} \end{array} \right\} \approx (0.8\ \text{GeV})^2$$

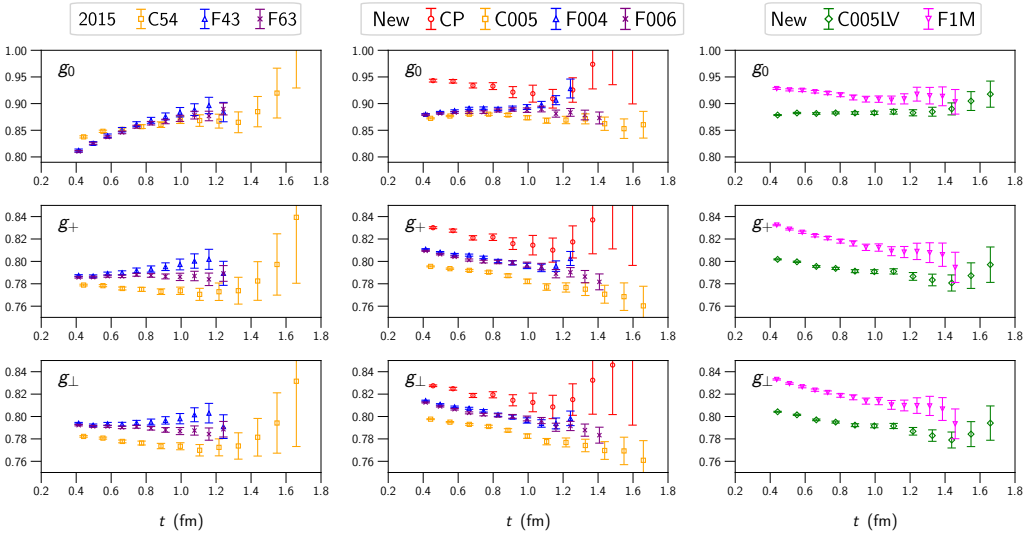

Preliminary results: $\Lambda_b \to \Lambda$

$$|\mathbf{p}'|^2 = \left\{ \begin{array}{ll} 3 \cdot (2\pi/L)^2 & \text{for C005, F004, F006,} \\ 12 \cdot (2\pi/L)^2 & \text{for CP,} \\ 5 \cdot (2\pi/L)^2 & \text{for C005LV, F1M} \end{array} \right\} \approx (0.8\ \text{GeV})^2$$

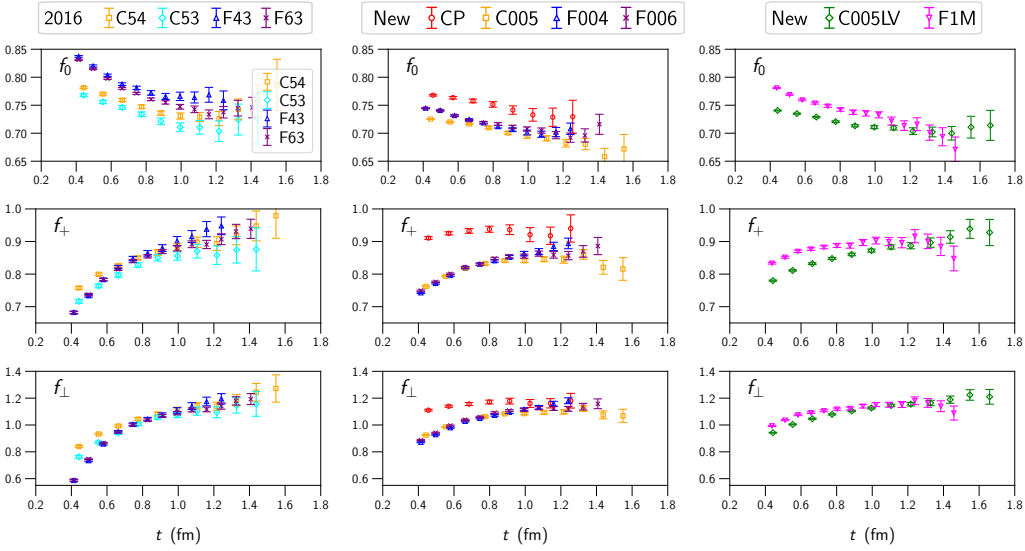

Preliminary results: $\Lambda_b \to \Lambda$

$$|\mathbf{p}'|^2 = \left\{ \begin{array}{ll} 3 \cdot (2\pi/L)^2 & \text{for C005, F004, F006,} \\ 12 \cdot (2\pi/L)^2 & \text{for CP,} \\ 5 \cdot (2\pi/L)^2 & \text{for C005LV, F1M} \end{array} \right\} \approx (0.8\ \text{GeV})^2$$

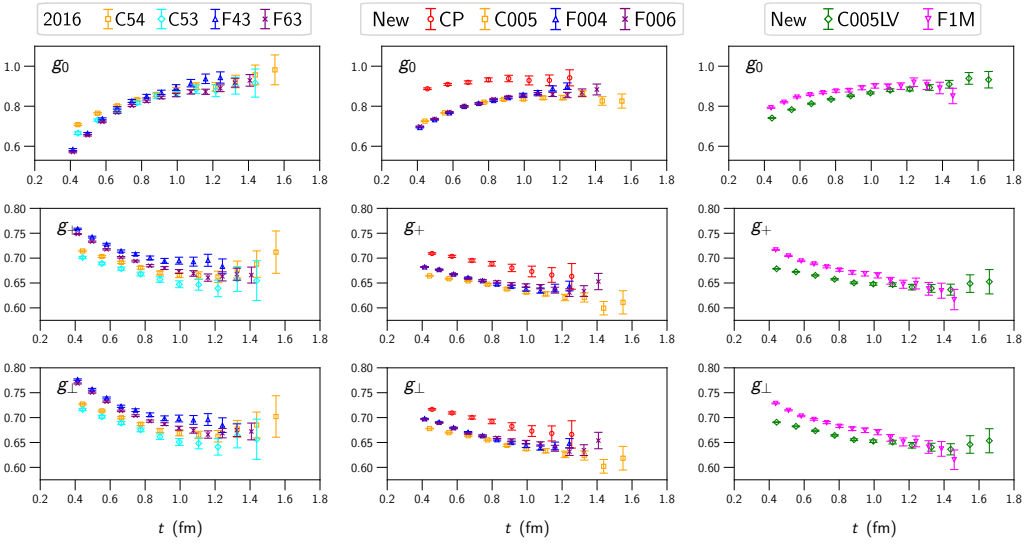

Preliminary results: $\Lambda_b \to p$

$$|\mathbf{p}'|^2 = \left\{ \begin{array}{ll} 3 \cdot (2\pi/L)^2 & \text{for C005, F004, F006,} \\ 12 \cdot (2\pi/L)^2 & \text{for CP,} \\ 5 \cdot (2\pi/L)^2 & \text{for C005LV, F1M} \end{array} \right\} \approx (0.8\ \text{GeV})^2$$

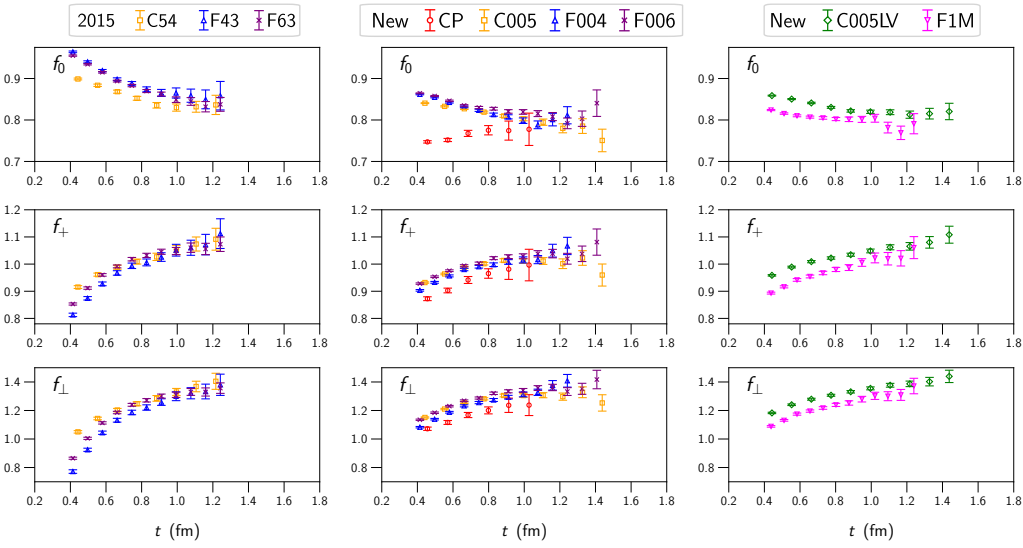

Preliminary results: $\Lambda_b \to p$

$$|\mathbf{p}'|^2 = \left\{ \begin{array}{ll} 3 \cdot (2\pi/L)^2 & \text{for C005, F004, F006,} \\ 12 \cdot (2\pi/L)^2 & \text{for CP,} \\ 5 \cdot (2\pi/L)^2 & \text{for C005LV, F1M} \end{array} \right\} \approx (0.8\ \text{GeV})^2$$

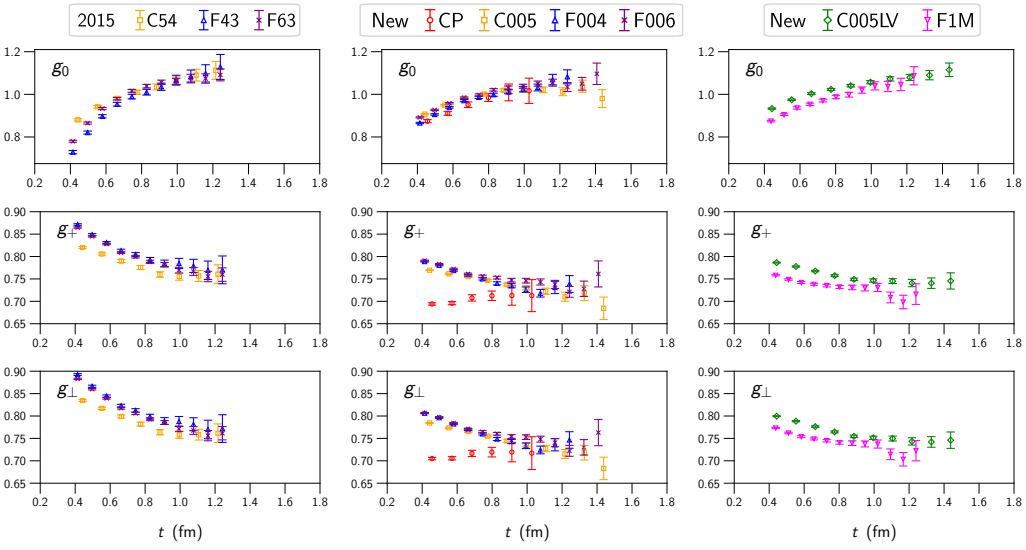

Next steps

- Complete the update of the renormalization factors and $O(a)$ improvement coefficients, possibly using a new fully nonperturbative method [D. Giusti and C. Lehner, 2111.15614/PoS Lattice 2021].
- Finalize the fits of the t-dependence of the $R_f(t)$ to extract the form-factor data points for all ensembles and all kinematic points.
- Perform the chiral/continuum/kinematic extrapolations. For the kinematic extrapolations, I plan to consider dispersive bounds.

Dispersive bounds on Λ_b semileptonic form factors

[T. Blake, S. Meinel, M. Rahimi, D. van Dyk, 2205.06041]

For definiteness we consider $\Lambda_b \to \Lambda$. An example of a dispersive bound is

$$\underbrace{\chi_V^{J=1}(Q^2)\Big|_{\text{OPE}}}_{\text{perturbation theory}} \geq \int_{t_{\text{th}}}^{\infty} \mathrm{d}t\, \frac{1}{24\pi^2} \frac{\sqrt{\lambda(m_{\Lambda_b}^2, m_\Lambda^2, t)}}{t^2(t-Q^2)^{n+1}} s_-(t) \left((m_{\Lambda_b} + m_\Lambda)^2 |f_+(t)|^2 + 2t|f_\perp(t)|^2 \right),$$

where $t_{\text{th}} = (m_{\Lambda_b} + m_\Lambda)^2$.

NB: 2205.06041 uses different names for the form factors, such as $(f_0^V, f_\perp^V, f_t^V)$ instead of $(f_+, f_\perp, f_0)$, but the definitions are identical. I have changed the names here to match the notation in the rest of the talk.

Dispersive bounds on Λ_b semileptonic form factors

The form factors have a branch cut starting at $t_+ = (m_B + m_K)^2$. We define the variable

$$z(t; t_0, t_+) = \frac{\sqrt{t_+ - t} - \sqrt{t_+ - t_0}}{\sqrt{t_+ - t} + \sqrt{t_+ - t_0}}.$$

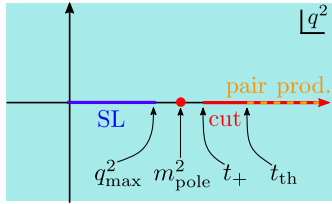

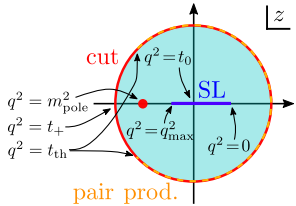

Then the dispersive bound can be written as

$$1 \geq \int_{-\alpha_{\Lambda_b\Lambda}}^{+\alpha_{\Lambda_b\Lambda}} \mathrm{d}\alpha \left(|\phi_{f_+}(z)|^2 |f_+(z)|^2 + |\phi_{f_\perp}(z)|^2 |f_\perp(z)|^2 \right)_{z=e^{i\alpha}}$$

where the ϕ's are the *outer functions* and

$$\alpha_{\Lambda_b\Lambda} = \arg z((m_\Lambda + m_{\Lambda_b})^2).$$

Dispersive bounds on Λ_b semileptonic form factors

The BGL z-expansion parametrization would be

$$f(q^2) = \frac{1}{\mathcal{P}(q^2)\,\phi_f(z)} \sum_{i=0}^{N} a_{f,i}\, z^i,$$

where $\mathcal{P}(q^2) = z(q^2; t_0 = m^2_{\text{pole}}, t_+)$ is the Blaschke factor. If we had $t_{\text{th}} = t_+$, so that the dispersive integral would go over the entire unit circle, we would have $1 \geq \sum_i (a^2_{f_+,i} + a^2_{f_\perp,i})$.

Dispersive bounds on Λ_b semileptonic form factors

The BGL z-expansion parametrization would be

$$f(q^2) = \frac{1}{\mathcal{P}(q^2)\,\phi_f(z)} \sum_{i=0}^{N} a_{f,i}\, z^i,$$

where $\mathcal{P}(q^2) = z(q^2; t_0 = m_{\text{pole}}^2, t_+)$ is the Blaschke factor. If we had $t_{\text{th}} = t_+$, so that the dispersive integral would go over the entire unit circle, we would have $1 \geq \sum_i (a_{f_+,i}^2 + a_{f_\perp,i}^2)$. But recall that

$$t_+ = (m_B + m_K)^2 < t_{\text{th}} = (m_{\Lambda_b} + m_\Lambda)^2,$$

so the integral only goes over an arc of the unit circle. To bring the bound into the form $1 \geq \sum_i (a_{f_+,i}^2 + a_{f_\perp,i}^2)$, we instead use the parametrization

$$f(q^2) = \frac{1}{\mathcal{P}(q^2)\,\phi_f(z)} \sum_{i=0}^{N} a_{f,i}|_N\, p_i(z),$$

where the $p_i(z)$ are orthonormal polynomials on that arc:

$$\int_{-\alpha_{\Lambda_b\Lambda}}^{+\alpha_{\Lambda_b\Lambda}} \mathrm{d}\alpha\; p_n^*(z)\, p_m(z)\big|_{z=e^{i\alpha}} = \delta_{nm}.$$

The polynomials $p_n(z)$ are *Szegő polynomials*. Note that in general any two sets of coefficients $\{a_{f,i}\}|_N$ and $\{a_{f,i}\}|_{N'}$ are not nested, i.e., the first $\min(N, N')$ elements of the sets are *not* identical.

Dispersive bounds on Λ_b semileptonic form factors

We tested the method using synthetic data points from the 2016 lattice results. The dispersive bounds allow stable extrapolations to low q^2.

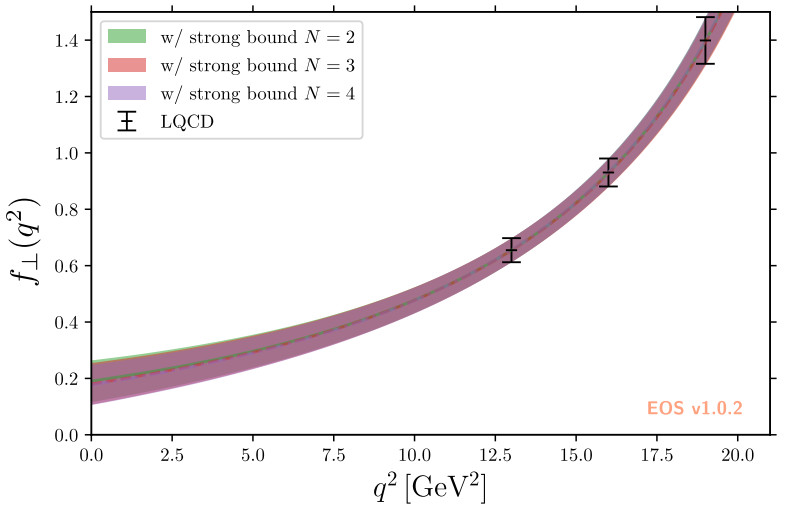

Summary

- Next-generation computations of the correlation functions needed to determine the $\Lambda_b \to p, \Lambda, \Lambda_c$ form factors have been completed.

- The new calculations include three additional ensembles (one with 139 MeV pion mass, one with 0.73 fm lattice spacing, and one with another volume) and were performed with a more accurate tuning of the charm and bottom anisotropic clover action parameters.

- The remaining tasks are
  - Complete the update of the renormalization factors and $O(a)$ improvement coefficients
  - Finalize the fits of the t-dependence of the $R_f(t)$ to extract the form-factor data points
  - Perform the chiral/continuum/kinematic extrapolations

- The benefit of dispersive bounds for kinematic extrapolations of the $\Lambda_b \to \Lambda$ form factors was demonstrated. The method uses a generalization of the z expansion suitable for cases with sub-threshold branch cuts (see also J. Flynn, A. Jüttner, J. Tsang, 2303.11285 and Andreas Jüttner's talk for an equivalent approach).

Extra slides: origin of the tension
in the heavy-quark parameter tuning

We write the $B_s^{(*)}$ dispersion relation as $(aE)^2 = (aM_{\text{rest}})^2 + \underbrace{\left(\frac{M_{\text{rest}}}{M_{\text{kin}}}\right)}_{\equiv c^2}(a\mathbf{p})^2$.

RBC/UKQCD determined c^2 as the slope of a linear fit to the $(aE)^2$ at $\mathbf{p}^2 = \{0, 1, 2, 3\}\left(\frac{2\pi}{L}\right)^2$. Their effective-energy plots of the two-point functions are shown below [Y. Aoki *et al.*, 1206.2554/PRD 2012]:

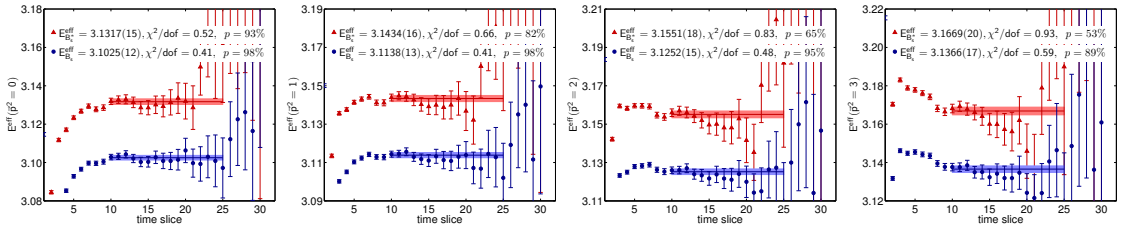

(these plots are for $\{am_Q, \nu, c_{E,B}\} = \{8.40, 3.20, 5.80\}$ on the $24^3 \times 64$ lattice)

When computing the very small differences in $(aE)^2$ between zero and nonzero momentum, and hence the slope, there is a large cancellation in statistical uncertainties due to correlations. However, we see in the figures above that, for the chosen smearings (strange quark: point source, point sink; bottom quark: smeared source, point sink), the excited-state contamination in $(aE)^2$ changes sign from negative to positive as $\mathbf{p}^2$ is increased. Thus, the excited-state contamination in the slope is *enhanced* and leads to an overestimate of c^2.

I used a different smearing scheme, with all quarks Gaussian-smeared at both source and sink (narrow width for b, broader width for s). Here is an example of the resulting pseudoscalar-B_s effective energies:

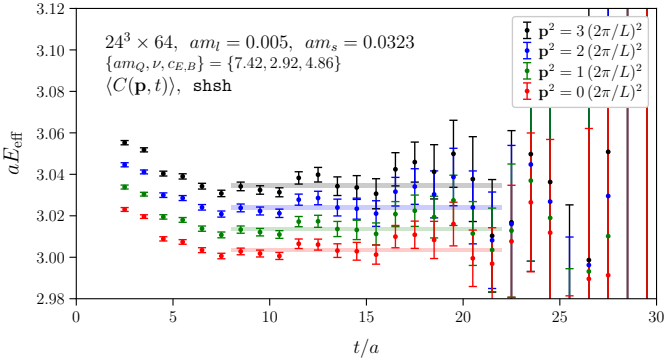

With this choice of smearings, the excited-state contamination is observed to be almost independent of $\mathbf{p}$.

(I find that this is still the case when using a point sink for just the strange quark while keeping a smeared sink for the bottom quark.)

Another way to see the stability is to look at the effective-energy plots of the ratios of two-point functions: